Diffractive Dijets with a Leading Antiproton in $\bar{p}p$ Collisions at $\sqrt{s} = 1800$ GeV

T. Affolder,[21] H. Akimoto,[43] A. Akopian,[36] M. G. Albrow,[10] P. Amaral,[7] S. R. Amendolia,[32] D. Amidei,[24] K. Anikeev,[22] J. Antos,[1] G. Apollinari,[36] T. Arisawa,[43] T. Asakawa,[41] W. Ashmanskas,[7] M. Atac,[10] F. Azfar,[29] P. Azzi-Bacchetta,[30] N. Bacchetta,[30] M. W. Bailey,[26] S. Bailey,[14] P. de Barbaro,[35] A. Barbaro-Galtieri,[21] V. E. Barnes,[34] B. A. Barnett,[17] M. Barone,[12] G. Bauer,[22] F. Bedeschi,[32] S. Belforte,[40] G. Bellettini,[32] J. Bellinger,[44] D. Benjamin,[9] J. Bensinger,[4] A. Beretvas,[10] J. P. Berge,[10] J. Berryhill,[7] B. Bevensee,[31] A. Bhatti,[36] M. Binkley,[10] D. Bisello,[30] R. E. Blair,[2] C. Blocker,[4] K. Bloom,[24] B. Blumenfeld,[17] S. R. Blusk,[35] A. Bocci,[32] A. Bodek,[35] W. Bokhari,[31] G. Bolla,[34] Y. Bonushkin,[5] K. Borras,[36] D. Bortoletto,[34] J. Boudreau,[33] A. Brandl,[26] S. van den Brink,[17] C. Bromberg,[25] M. Brozovic,[9] N. Bruner,[26] E. Buckley-Geer,[10] J. Budagov,[8] H. S. Budd,[35] K. Burkett,[14] G. Busetto,[30] A. Byon-Wagner,[10] K. L. Byrum,[2] M. Campbell,[24] W. Carithers,[21] J. Carlson,[24] D. Carlsmith,[44] J. Cassada,[35] A. Castro,[30] D. Cauz,[40] A. Cerri,[32] A. W. Chan,[1] P. S. Chang,[1] P. T. Chang,[1] J. Chapman,[24] C. Chen,[31] Y. C. Chen,[1] M.-T. Cheng,[1] M. Chertok,[38] G. Chiarelli,[32] I. Chirikov-Zorin,[8] G. Chlachidze,[8] F. Chlebana,[10] L. Christofek,[16] M. L. Chu,[1] S. Cihangir,[10] C. I. Ciobanu,[27] A. G. Clark,[13] A. Connolly,[21] M. Convery,[36] J. Conway,[37] J. Cooper,[10] M. Cordelli,[12] J. Cranshaw,[39] D. Cronin-Hennessy,[9] R. Cropp,[23] R. Culbertson,[7] D. Dagenhart,[42] F. DeJongh,[10] S. Dell'Agnello,[12] M. Dell'Orso,[32] R. Demina,[10] L. Demortier,[36] M. Deninno,[3] P. F. Derwent,[10] T. Devlin,[37] J. R. Dittmann,[10] S. Donati,[32] J. Done,[38] T. Dorigo,[14] N. Eddy,[16] K. Einsweiler,[21] J. E. Elias,[10] E. Engels, Jr.,[33] W. Erdmann,[10] D. Errede,[16] S. Errede,[16] Q. Fan,[35] R. G. Feild,[45] C. Ferretti,[32] R. D. Field,[11] I. Fiori,[3] B. Flaugher,[10] G. W. Foster,[10] M. Franklin,[14] J. Freeman,[10] J. Friedman,[22] Y. Fukui,[20] S. Galeotti,[32] M. Gallinaro,[36] T. Gao,[31] M. Garcia-Sciveres,[21] A. F. Garfinkel,[34] P. Gatti,[30] C. Gay,[45] S. Geer,[10] D. W. Gerdes,[24] P. Giannetti,[32] V. Glagolev,[8] M. Gold,[26] J. Goldstein,[10] A. Gordon,[14] A. T. Goshaw,[9] Y. Gotra,[33] K. Goulianos,[36] C. Green,[34] L. Groer,[37] C. Grosso-Pilcher,[7] M. Guenther,[34] G. Guillian,[24] J. Guimaraes da Costa,[24] R. S. Guo,[1] C. Haber,[21] E. Hafen,[22] S. R. Hahn,[10] C. Hall,[14] T. Handa,[15] R. Handler,[44] W. Hao,[39] F. Happacher,[12] K. Hara,[41] A. D. Hardman,[34] R. M. Harris,[10] F. Hartmann,[18] K. Hatakeyama,[36] J. Hauser,[5] J. Heinrich,[31] A. Heiss,[18] M. Herndon,[17] B. Hinrichsen,[23] K. D. Hoffman,[34] C. Holck,[31] R. Hollebeek,[31] L. Holloway,[16] R. Hughes,[27] J. Huston,[25] J. Huth,[14] H. Ikeda,[41] J. Incandela,[10] G. Introzzi,[32] J. Iwai,[43] Y. Iwata,[15] E. James,[24] H. Jensen,[10] M. Jones,[31] U. Joshi,[10] H. Kambara,[13] T. Kamon,[38] T. Kaneko,[41] K. Karr,[42] H. Kasha,[45] Y. Kato,[28] T. A. Keaffaber,[34] K. Kelley,[22] M. Kelly,[24] R. D. Kennedy,[10] R. Kephart,[10] D. Khazins,[9] T. Kikuchi,[41] M. Kirk,[4] B. J. Kim,[19] H. S. Kim,[16] M. J. Kim,[19] S. H. Kim,[41] Y. K. Kim,[21] L. Kirsch,[4] S. Klimenko,[11] P. Koehn,[27] A. Köngeter,[18] K. Kondo,[43] J. Konigsberg,[11] K. Kordas,[23] A. Korn,[22] A. Korytov,[11] E. Kovacs,[2] J. Kroll,[31] M. Kruse,[35] S. E. Kuhlmann,[2] K. Kurino,[15] T. Kuwabara,[41] A. T. Laasanen,[34] N. Lai,[7] S. Lami,[36] S. Lammel,[10] J. I. Lamoureux,[4] M. Lancaster,[21] G. Latino,[32] T. LeCompte,[2] A. M. Lee IV,[9] S. Leone,[32] J. D. Lewis,[10] M. Lindgren,[5] T. M. Liss,[16] J. B. Liu,[35] Y. C. Liu,[1] N. Lockyer,[31] J. Loken,[29] M. Loreti,[30] D. Lucchesi,[30] P. Lukens,[10] S. Lusin,[44] L. Lyons,[29] J. Lys,[21] R. Madrak,[14] K. Maeshima,[10] P. Maksimovic,[14] L. Malferrari,[3] M. Mangano,[32] M. Mariotti,[30] G. Martignon,[30] A. Martin,[45] J. A. J. Matthews,[26] J. Mayer,[23] P. Mazzanti,[3] K. S. McFarland,[35] P. McIntyre,[38] E. McKigney,[31] P. Melese,[36] M. Menguzzato,[30] A. Menzione,[32] C. Mesropian,[36] T. Miao,[10] R. Miller,[25] J. S. Miller,[24] H. Minato,[41] S. Miscetti,[12] M. Mishina,[20] G. Mitselmakher,[11] N. Moggi,[3] C. Moore,[10] E. Moore,[26] R. Moore,[24] Y. Morita,[20] A. Mukherjee,[10] T. Muller,[18] A. Munar,[32] P. Murat,[10] S. Murgia,[25] M. Musy,[40] J. Nachtman,[5] S. Nahn,[45] H. Nakada,[41] T. Nakaya,[7] I. Nakano,[15] C. Nelson,[10] D. Neuberger,[18] C. Newman-Holmes,[10] C.-Y. P. Ngan,[22] P. Nicolaidi,[40] H. Niu,[4] L. Nodulman,[2] A. Nomerotski,[11] S. H. Oh,[9] T. Ohmoto,[15] T. Ohsugi,[15] R. Oishi,[41] T. Okusawa,[28] J. Olsen,[44] C. Pagliarone,[32] F. Palmonari,[32] R. Paoletti,[32] V. Papadimitriou,[39] S. P. Pappas,[45] D. Partos,[4] J. Patrick,[10] G. Pauletta,[40] M. Paulini,[21] C. Paus,[22] L. Pescara,[30] T. J. Phillips,[9] G. Piacentino,[32] K. T. Pitts,[16] R. Plunkett,[10] A. Pompos,[34] L. Pondrom,[44] G. Pope,[33] M. Popovic,[23] F. Prokoshin,[8] J. Proudfoot,[2] F. Ptohos,[12] G. Punzi,[32] K. Ragan,[23] A. Rakitine,[22] D. Reher,[21] A. Reichold,[29] W. Riegler,[14] A. Ribon,[30] F. Rimondi,[3] L. Ristori,[32] W. J. Robertson,[9] A. Robinson,[23] T. Rodrigo,[6] S. Rolli,[42] L. Rosenson,[22] R. Roser,[10] R. Rossin,[30] W. K. Sakumoto,[35] D. Saltzberg,[5] A. Sansoni,[12] L. Santi,[40] H. Sato,[41] P. Savard,[23] P. Schlabach,[10] E. E. Schmidt,[10] M. P. Schmidt,[45] M. Schmitt,[14] L. Scodellaro,[30] A. Scott,[5] A. Scribano,[32] S. Segler,[10] S. Seidel,[26] Y. Seiya,[41] A. Semenov,[8] F. Semeria,[3] T. Shah,[22] M. D. Shapiro,[21] P. F. Shepard,[33] T. Shibayama,[41] M. Shimojima,[41] M. Shochet,[7] J. Siegrist,[21] G. Signorelli,[32] A. Sill,[39] P. Sinervo,[23] P. Singh,[16] A. J. Slaughter,[45] K. Sliwa,[42] C. Smith,[17] F. D. Snider,[10] A. Solodsky,[36] J. Spalding,[10] T. Speer,[13] P. Sphicas,[22] F. Spinella,[32] M. Spiropulu,[14] L. Spiegel,[10] J. Steele,[44] A. Stefanini,[32] J. Strologas,[16] F. Strumia,[13] D. Stuart,[10] K. Sumorok,[22] T. Suzuki,[41] T. Takano,[28]

R. Takashima,[15] K. Takikawa,[41] P. Tamburello,[9] M. Tanaka,[41] B. Tannenbaum,[5] W. Taylor,[23] M. Tecchio,[24] P. K. Teng,[1] K. Terashi,[41] S. Tether,[22] D. Theriot,[10] R. Thurman-Keup,[2] P. Tipton,[35] S. Tkaczyk,[10] K. Tollefson,[35] A. Tollestrup,[10] H. Toyoda,[28] W. Trischuk,[23] J. F. de Troconiz,[14] J. Tseng,[22] N. Turini,[32] F. Ukegawa,[41] T. Vaiciulis,[35] J. Valls,[37] S. Vejcik III,[10] G. Velev,[10] R. Vidal,[10] R. Vilar,[6] I. Volobouev,[21] D. Vucinic,[22] R. G. Wagner,[2] R. L. Wagner,[10] J. Wahl,[7] N. B. Wallace,[37] A. M. Walsh,[37] C. Wang,[9] C. H. Wang,[1] M. J. Wang,[1] T. Watanabe,[41] D. Waters,[29] T. Watts,[37] R. Webb,[38] H. Wenzel,[18] W. C. Wester III,[10] A. B. Wicklund,[2] E. Wicklund,[10] H. H. Williams,[31] P. Wilson,[10] B. L. Winer,[27] D. Winn,[24] S. Wolbers,[10] D. Wolinski,[24] J. Wolinski,[25] S. Wolinski,[24] S. Worm,[26] X. Wu,[13] J. Wyss,[32] A. Yagil,[10] W. Yao,[21] G. P. Yeh,[10] P. Yeh,[1] J. Yoh,[10] C. Yosef,[25] T. Yoshida,[28] I. Yu,[19] S. Yu,[31] A. Zanetti,[40] F. Zetti,[21] and S. Zucchelli[3]

(CDF Collaboration)

[1]*Institute of Physics, Academia Sinica, Taipei, Taiwan 11529, Republic of China*
[2]*Argonne National Laboratory, Argonne, Illinois 60439*
[3]*Istituto Nazionale di Fisica Nucleare, University of Bologna, I-40127 Bologna, Italy*
[4]*Brandeis University, Waltham, Massachusetts 02254*
[5]*University of California at Los Angeles, Los Angeles, California 90024*
[6]*Instituto de Fisica de Cantabria, University of Cantabria, 39005 Santander, Spain*
[7]*Enrico Fermi Institute, University of Chicago, Chicago, Illinois 60637*
[8]*Joint Institute for Nuclear Research, RU-141980 Dubna, Russia*
[9]*Duke University, Durham, North Carolina 27708*
[10]*Fermi National Accelerator Laboratory, Batavia, Illinois 60510*
[11]*University of Florida, Gainesville, Florida 32611*
[12]*Laboratori Nazionali di Frascati, Istituto Nazionale di Fisica Nucleare, I-00044 Frascati, Italy*
[13]*University of Geneva, CH-1211 Geneva 4, Switzerland*
[14]*Harvard University, Cambridge, Massachusetts 02138*
[15]*Hiroshima University, Higashi-Hiroshima 724, Japan*
[16]*University of Illinois, Urbana, Illinois 61801*
[17]*The Johns Hopkins University, Baltimore, Maryland 21218*
[18]*Institut für Experimentelle Kernphysik, Universität Karlsruhe, 76128 Karlsruhe, Germany*
[19]*Korean Hadron Collider Laboratory, Kyungpook National University, Taegu 702-701, Korea and Seoul National University, Seoul 151-742, Korea and SungKyunKwan University, Suwon 440-746, Korea*
[20]*High Energy Accelerator Research Organization (KEK), Tsukuba, Ibaraki 305, Japan*
[21]*Ernest Orlando Lawrence Berkeley National Laboratory, Berkeley, California 94720*
[22]*Massachusetts Institute of Technology, Cambridge, Massachusetts 02139*
[23]*Institute of Particle Physics, McGill University, Montreal, Canada H3A 2T8 and University of Toronto, Toronto, Canada M5S 1A7*
[24]*University of Michigan, Ann Arbor, Michigan 48109*
[25]*Michigan State University, East Lansing, Michigan 48824*
[26]*University of New Mexico, Albuquerque, New Mexico 87131*
[27]*The Ohio State University, Columbus, Ohio 43210*
[28]*Osaka City University, Osaka 588, Japan*
[29]*University of Oxford, Oxford OX1 3RH, United Kingdom*
[30]*Universita di Padova, Istituto Nazionale di Fisica Nucleare, Sezione di Padova, I-35131 Padova, Italy*
[31]*University of Pennsylvania, Philadelphia, Pennsylvania 19104*
[32]*Istituto Nazionale di Fisica Nucleare, University and Scuola Normale Superiore of Pisa, I-56100 Pisa, Italy*
[33]*University of Pittsburgh, Pittsburgh, Pennsylvania 15260*
[34]*Purdue University, West Lafayette, Indiana 47907*
[35]*University of Rochester, Rochester, New York 14627*
[36]*Rockefeller University, New York, New York 10021*
[37]*Rutgers University, Piscataway, New Jersey 08855*
[38]*Texas A&M University, College Station, Texas 77843*
[39]*Texas Tech University, Lubbock, Texas 79409*
[40]*Istituto Nazionale di Fisica Nucleare, University of Trieste, Udine, Italy*
[41]*University of Tsukuba, Tsukuba, Ibaraki 305, Japan*
[42]*Tufts University, Medford, Massachusetts 02155*
[43]*Waseda University, Tokyo 169, Japan*
[44]*University of Wisconsin, Madison, Wisconsin 53706*
[45]*Yale University, New Haven, Connecticut 06520*

(Received 6 March 2000)

We report results from a study of events with a leading antiproton of beam momentum fraction $0.905 < x_F < 0.965$ and 4-momentum transfer squared $|t| < 3$ GeV^2 produced in $\bar{p}p$ collisions at $\sqrt{s} = 1800$ GeV at the Fermilab Tevatron collider. Approximately 2% of the events contain two jets of transverse energy $E_T^{\text{jet}} > 7$ GeV. Using the dijet events, we evaluate the diffractive structure function of the antiproton and compare it with expectations based on results obtained in diffractive deep inelastic scattering experiments at the DESY ep collider HERA.

PACS numbers: 13.87.Ce, 12.38.Qk, 12.40.Nn

Experiments at the DESY ep collider HERA [1,2] and at $\bar{p}p$ colliders [3,4] have reported and characterized events containing a hard scattering while carrying the characteristic signature of single diffraction dissociation, namely, a leading (anti)proton and/or a forward rapidity gap. The prevailing theoretical concept is that the rapidity gap, defined as a region of pseudorapidity [5] devoid of particles, is associated with the exchange of a Pomeron ($I\!P$) [6], which in QCD is a color-singlet state with vacuum quantum numbers. In this framework, $\bar{p}p$ *hard diffraction* can be expressed as a two-step process, $\bar{p} + p \to [\bar{p}' + I\!P] + p \to \bar{p}' + (W, \text{dijet}, \ldots) + X$, and similarly, diffractive deep inelastic scattering (DDIS) as $\gamma^* + p \to \gamma^* + [p' + I\!P] \to p' + X$.

The central issue in this field is whether hard diffraction processes obey QCD factorization, i.e., can be described in terms of parton level cross sections convoluted with a universal "diffractive" (anti)proton structure function. In addition to its usual dependence on x-Bjorken and Q^2, the diffractive structure function could also depend on the recoil (anti)proton fractional momentum loss ξ and 4-momentum transfer squared t. The DDIS experiments measure the diffractive structure function of the proton, $F_2^{D(3)}(\xi, \beta, Q^2)$, integrated over t, where $\beta \equiv x/\xi$ may be interpreted as the momentum fraction of the parton in the Pomeron and Q^2 is the virtuality of γ^*. Diffractive quark densities are obtained directly from $F_2^{D(3)}(\xi, \beta, Q^2)$. Using a QCD analysis, the H1 Collaboration derived [1] diffractive gluon densities from the observed Q^2 dependence of $F_2^{D(3)}$. The HERA data, including hard photoproduction, are generally consistent with the parton densities extracted by the H1 analysis. However, calculations of W and dijet production rates at the Tevatron using the H1 parton densities predict [7–9] rates $\sim$10 times larger than those measured. The observed discrepancy challenges the universality of the diffractive parton densities extracted from DDIS and leads naturally to the question of whether the shape of the β distribution is also process dependent. In the present experiment, we measure both the shape and absolute normalization of the antiproton diffractive structure function in events with two jets and a leading antiproton produced in $\bar{p}p$ collisions at $\sqrt{s} = 1800$ GeV, and test factorization by comparing our results with expectations based on the diffractive proton structure function determined in DDIS.

Our experimental procedure may be outlined as follows. From an inclusive sample of single diffraction (SD) events, $\bar{p}p \to \bar{p}'X$, collected by the CDF detector by triggering on a $\bar{p}$ detected in a forward magnetic "Roman pot" spectrometer (RPS), we select a diffractive dijet subsample, $\bar{p} + p \to \bar{p}' + \text{Jet}_1 + \text{Jet}_2 + X$, containing two jets with transverse energy [5] $E_T^{\text{jet}} > 7$ GeV. In addition to the two *leading* jets, the event may contain other (lower E_T) jets. Similarly, a nondiffractive (ND) dijet sample is selected from events collected with a minimum bias (MB) trigger requiring a coincidence between two beam-beam counter (BBC) arrays [10] covering the region $3.2 < |\eta| < 5.9$. From the E_T and η of the jets we evaluate the fraction x of the momentum of the antiproton carried by the struck parton,

$$x = \frac{1}{\sqrt{s}} \sum_{i=1}^{n} E_T^i e^{-\eta^i},$$

where the sum is carried over the two leading jets plus the next highest E_T jet, if there is one with $E_T > 5$ GeV. In leading order QCD, the ratio $R(x)$ of the SD to ND rates is equal to the ratio of the antiproton SD to ND structure functions. Thus, the diffractive structure function may be obtained by multiplying the known ND structure function by $R(x)$. The absolute normalization of the SD dijet sample is obtained by scaling the event rate to that of the inclusive diffractive sample and using for the latter our previously measured inclusive cross section [11]. The normalization of the ND dijet sample is obtained from the measured 51.2 ± 1.7 mb cross section of the BBC trigger.

The CDF detector is described elsewhere [10]. The jets were detected and their energy measured by calorimeters covering the pseudorapidity range $|\eta| < 4.2$. The position of the event vertex was determined from the tracks registered in the central tracking detectors. During the Tevatron collider run of 1995–1996 (Run 1C), in which the present data sample was collected, the RPS was added to CDF. It consisted of X-Y scintillation fiber tracking detectors placed in Roman pot vessels attached to the machine vacuum pipe by bellows, so that they could be moved remotely to bring the detectors close to the circulating beams after attaining stable beam conditions, as described in [11]. The spectrometer comprised three Roman pots, spaced $\sim$1 m apart from one another along the beam direction. The pots were positioned on the inside of the Tevatron ring in a straight section of the machine located $\sim$57 m downstream in the $\bar{p}$ beam direction, following a string of dipole magnets. In addition to the X-Y fiber tracker, each pot contained a scintillation counter used for triggering. A coincidence among the trigger counters of the three Roman pots, in time with a $\bar{p}$ gate, provided the inclusive

diffractive trigger. The momentum and t value of the detected antiproton were determined from a fit to the X-Y Roman pot track positions and the vertex of the event, using the beam transport matrix in the fit. The Roman pot position resolution was $\pm 100\ \mu$m. In the region of our measurement, typical resolutions in ξ and t were $\delta\xi = \pm 0.001$ and $\delta t = \pm 0.07\ \mathrm{GeV}^2$.

The data were collected during runs of typical luminosities $\sim 3 \times 10^{29}\ \mathrm{cm}^{-2}\,\mathrm{sec}^{-1}$. After applying off-line cuts requiring a reconstructed track with acceptable χ^2 traversing all three Roman pot detectors, and a single reconstructed vertex within $|z_{\mathrm{vtx}}| < 60$ cm, we obtained 1.6×10^6 SD events. From this *inclusive* data set, and a sample of 300 K MB events, we extracted two respective *dijet* subsamples, consisting of 30 410 SD and 32 629 ND events with two jets of corrected $E_T^{\mathrm{jet}} > 7$ GeV. The E_T^{jet} was defined as the sum of the calorimeter E_T within an η-ϕ cone of radius 0.7 [12]. The jet energy correction included subtraction of an average underlying event E_T of 0.54 (1.16) GeV for diffractive (nondiffractive) events. These values were determined experimentally, separately for SD and ND events, from the $\sum E_T$ of calorimeter tower energy measured within a randomly chosen η-ϕ cone of radius 0.7 in events of the inclusive data samples.

The diffractive dijet sample contains $(7.0 \pm 0.7)\%$ *overlap events*, consisting of a soft SD event superimposed on a ND dijet event. Such events are due to two $\bar{p}p$ interactions occurring in the same beam-bunch crossing at the detector. The fraction of overlap events was determined from an analysis of the BBC and forward calorimeter tower multiplicities. Each diffractive data distribution is corrected for the overlap background by subtracting the corresponding ND distribution normalized to the overlap fraction. Another correction is due to the single vertex selection requirement imposed on the SD data. In addition to rejecting events from multiple interactions, this requirement also rejects single interaction events with multiple vertices caused by reconstruction ambiguities in high multiplicity events. From an analysis of the BBC and forward calorimeter tower multiplicities, the single vertex cut efficiency (fraction of single interaction events retained by the single vertex cut) was determined to be $(81 \pm 2)\%$.

Figures 1(a) and 1(b) show, respectively, the RPS acceptance and a lego plot of the inclusive diffractive event sample as a function of ξ and t. The fraction of dijet events in the inclusive sample is shown as a function of ξ in Fig. 1(c) and versus t in Fig. 1(d). The fraction increases linearly as a function of ξ, but no significant t dependence is observed in agreement with the UA8 result [3] of a flat t dependence in the region $0.9 < |t| < 2.3$.

Figure 2 presents the dijet mean E_T and mean η distributions, $E_T^* = (E_T^{\mathrm{jet1}} + E_T^{\mathrm{jet2}})/2$ and $\eta^* = (\eta^{\mathrm{jet1}} + \eta^{\mathrm{jet2}})/2$, for the diffractive (points) and ND (histograms) event samples. The diffractive E_T^* distribution is somewhat steeper than the ND, and the diffractive η^* is boosted towards the proton direction (positive η^*). These

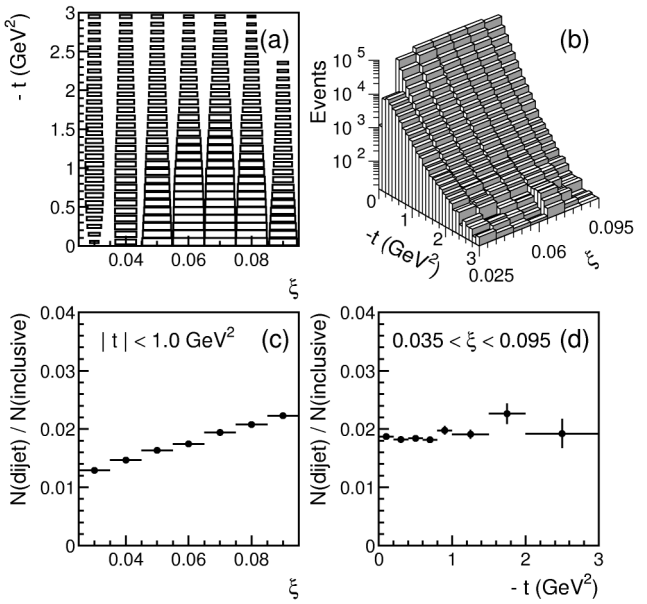

FIG. 1. Distributions versus ξ and t: (a) Roman pot acceptance; (b) inclusive diffractive event sample; (c) ratio of dijet to inclusive diffractive events versus ξ and (d) versus t.

features indicate that the x dependence of the diffractive structure function of the antiproton is steeper than that of the ND.

Figure 3 shows the ratio $\tilde{R}(x)$ of the number of SD dijet events, corrected for Roman pot acceptance, to the number of ND dijets, where the two data samples were normalized to correspond to the same luminosity. The tilde over the R indicates integration over all variables other than x within the region of the data samples under consideration, namely, $(t, \xi, E_T^{\mathrm{jet}})$ for diffractive and E_T^{jet} for ND events. The results are shown in Fig. 3 for $|t| < 1\ \mathrm{GeV}^2$ and $E_T(\mathrm{jet1}, \mathrm{jet2}) > 7$ GeV in six ξ bins of width $\Delta\xi = 0.01$ in the range $0.035 < \xi < 0.095$. The lines through the data points are fits of the form $\tilde{R}(x) = R_0(x/0.0065)^{-r}$ in the region $10^{-3} < x < 0.5\xi_{\mathrm{min}}$ for each ξ bin. The lower x limit is imposed to minimize the influence of detector end effects. As mentioned above, $R(x)$ represents the ratio

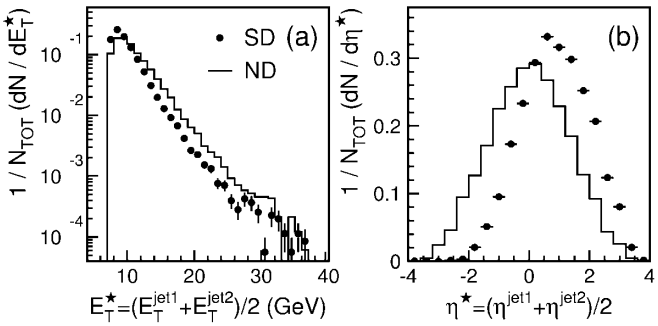

FIG. 2. Comparison of diffractive to nondiffractive dijet (a) mean E_T and (b) mean η distributions.

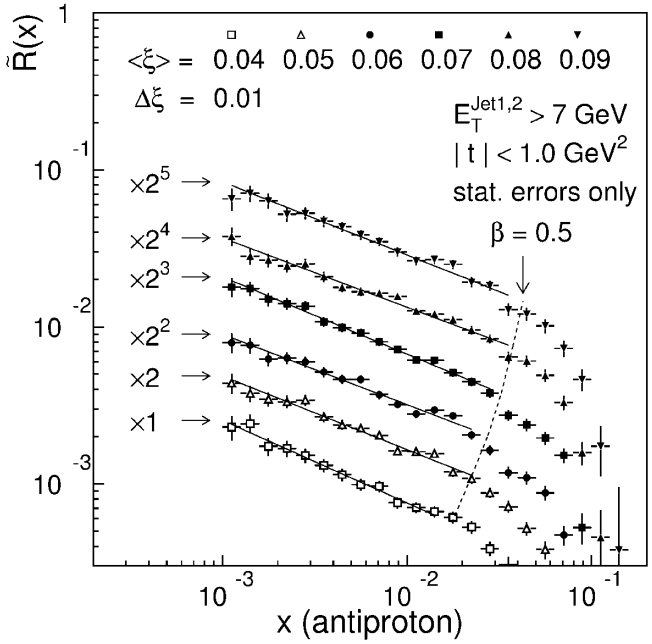

FIG. 3. Ratio of diffractive to nondiffractive dijet event rates as a function of x (momentum fraction of parton in $\bar{p}$). The solid lines are fits to the form $\tilde{R}(x) = R_0(x/0.0065)^{-r}$ for $\beta < 0.5$.

of the diffractive to ND parton densities of the antiproton, as "viewed" by dijet production. We will denote the associated structure functions by $F_{jj}(x) = x[g(x) + \frac{4}{9}q(x)]$, where $g(x)$ is the gluon and $q(x)$ is the quark density; the latter is multiplied by $\frac{4}{9}$ to account for color factors. The shape of the $\tilde{R}(x)$ distribution exhibits no significant ξ dependence. A fit to all the data in the region $0.035 < \xi < 0.095$ yields $R_0 = (6.1 \pm 0.1) \times 10^{-3}$ and $r = 0.45 \pm 0.02$ with $\chi^2/\text{d.o.f.} = 0.76$. The exponent r is insensitive to systematic uncertainties in jet energy calibration, which generally depend on η^{jet}. A 30% change in the SD or ND underlying event energy values results in a 14% change in R_0; adding in quadrature an estimated 20% normalization uncertainty yields an overall *systematic* uncertainty of $\pm 25\%$. Another uncertainty arises from the sensitivity of the parameters R_0 and r to the number of jets used in evaluating x. Using only the two leading jets yields $R_0 = (4.8 \pm 0.1) \times 10^{-3}$ and $r = 0.33 \pm 0.02$ ($\chi^2/\text{d.o.f.} = 1.21$), while by using up to four jets with $E_T > 5$ GeV we obtain $R_0 = (7.0 \pm 0.1) \times 10^{-3}$ and $r = 0.48 \pm 0.02$ ($\chi^2/\text{d.o.f.} = 0.74$). About 48% (23%) of the SD (ND) events have no jets of $E_T > 5$ GeV, other than the two leading jets; for these events $R_0 = (9.6 \pm 0.2) \times 10^{-3}$ and $r = 0.31 \pm 0.03$ ($\chi^2/\text{d.o.f.} = 1.18$).

The diffractive structure function of the antiproton is obtained from the equation

$$\tilde{F}_{jj}^D(\beta) = \tilde{R}(x = \beta\xi) \times \tilde{F}_{jj}^{ND}(x \to \beta\xi).$$

We have evaluated $\tilde{F}_{jj}^D(\beta)$ for $|t| < 1$ GeV^2, $0.035 < \xi < 0.095$, and $E_T(\text{jet1}, \text{jet2}) > 7$ GeV using the GRV98LO parton density set [13] in $\tilde{F}_{jj}^{ND}(x \to \beta\xi)$. The result is shown in Fig. 4. The solid curve is a fit to the data of the form $\tilde{F}_{jj}^D(\beta) = B(\beta/0.1)^{-n}$ in the range $(10^{-3}/\xi) < \beta < 0.5$, which corresponds to the region $10^{-3} < x < 0.5\xi_{\min}$ of Fig. 3. For our average ξ of 0.065 the value of $\beta = 0.1$, for which $\tilde{F}_{jj}^D = B$, corresponds to $x = 0.0065$, for which $\tilde{R} = R_0$. This fit yields $B = 1.12 \pm 0.01$ and $n = 1.08 \pm 0.01$ with $\chi^2/\text{d.o.f.} = 1.7$. The systematic uncertainty in B is ± 0.28, carried over from that in R_0. The lower and upper boundaries of the filled band surrounding the data points represent the β distributions obtained by using only the two leading jets or up to four jets of $E_T > 5$ GeV, respectively, in the evaluation of x. The dashed (dotted) curve is the expectation for $\tilde{F}_{jj}^D(\beta)$ calculated from fit 2 (fit 3) of the H1 diffractive structure function [1] evaluated at $Q^2 = 75$ GeV^2, which approximately corresponds to the average value of $(E_T^{\text{jet}})^2$ of our data. The H1 structure function, which was derived from data in the region of $\xi < 0.04$, has two terms, presumed to be due to Pomeron ($I\!P$) and Reggeon ($I\!R$) exchanges. Each term consists of the structure function of the exchanged Pomeron/Reggeon multiplied by the corresponding flux factor, $f_{(I\!P,I\!R)/\bar{p}}(\xi, t)$:

$$\tilde{F}_{jj}^D(\beta) = \sum_{i=I\!P,I\!R} \int_{t=-1}^{t_{\min}} \int_{\xi=0.035}^{\xi=0.095} C_i \cdot f_{i/\bar{p}}(\xi, t) \cdot F_{jj}^i(\beta)\, d\xi\, dt\,.$$

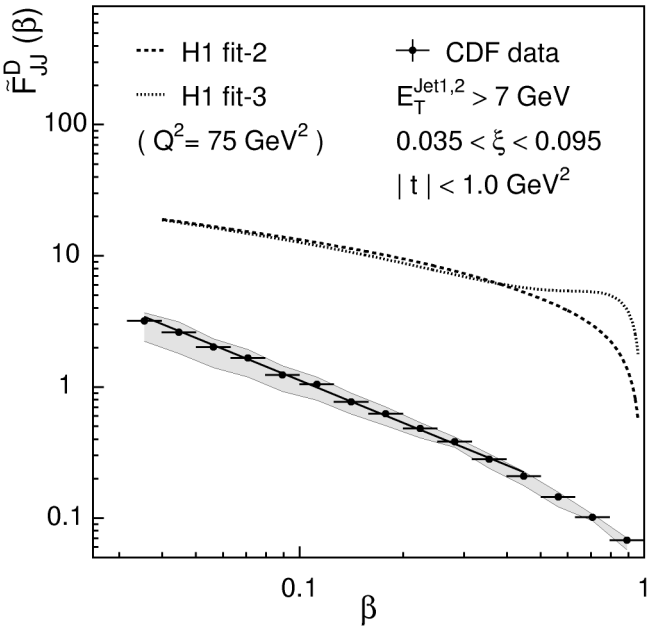

FIG. 4. Data β distribution (points) compared with expectations from the parton densities of the proton extracted from diffractive deep inelastic scattering by the H1 Collaboration. The straight line is a fit to the data of the form β^{-n}. The lower (upper) boundary of the filled band represents the data distribution obtained by using only the two leading jets (up to four jets of $E_T > 5$ GeV) in evaluating β. The dashed (dotted) lines are expectations from the H1 fit 2 (fit 3). The systematic uncertainty in the normalization of the data is $\pm 25\%$.

For the Pomeron we used parton densities from the H1 fits and for the Reggeon the Owens [14] pion structure; for the flux factors we used the form $f_{i/\bar{p}}(\xi, t) = e^{b_i t}/\xi^{2\alpha_i(t)-1}$ with the H1 fit parameters $\alpha_{I\!P}(t) = 1.20 + 0.26t$, $\alpha_{I\!R}(t) = 0.57 + 0.9t$, $b_{I\!P} = 4.6\ \mathrm{GeV}^{-2}$, $b_{I\!R} = 2.0\ \mathrm{GeV}^{-2}$, $C_{I\!P} = 1$, and $C_{I\!R} = 16.0$ (15.9) for fit 2 (fit 3) [15]. The measured and expected structure functions disagree both in normalization and shape. The discrepancy in normalization, defined as the ratio of the integral over β of data to expectation, is $D = 0.06 \pm 0.02$ (0.05 ± 0.02) for fit 2 (fit 3).

The disagreement between our measured diffractive structure function and the expectation from DDIS represents a breakdown of factorization. A similar breakdown was observed [4] in comparing diffractive W-boson and dijet production rates at the Tevatron with expectations based on ZEUS results [2] obtained from DDIS and dijet photoproduction at HERA. The normalization discrepancy in that case, based on comparisons made through Monte Carlo simulations, was found to be $D = 0.18 \pm 0.04$. The relative suppression of Tevatron to HERA diffractive rates is in general agreement with predictions based on the renormalized Pomeron flux [7,16] and soft color exchange [17] models.

In summary, we have studied the properties of dijet events of $E_T^{\mathrm{jet}} > 7$ GeV produced diffractively in $\bar{p}p$ collisions at $\sqrt{s} = 1800$ GeV in the range $0.035 < \xi < 0.095$ and $|t| < 3\ \mathrm{GeV}^2$ and determined the diffractive structure function of the antiproton, $\tilde{F}_{jj}^{D}(\beta)$, as a function of $\beta \equiv x(\text{parton in } \bar{p})/\xi$. The ratio of dijet to inclusive diffractive rates shows no significant t dependence. For $\beta < 0.5$, the β distribution of $\tilde{F}_{jj}^{D}(\beta)$ varies as $\sim 1/\beta$. Comparison of $\tilde{F}_{jj}^{D}(\beta)$ with expectations based on parton densities extracted from diffractive DIS at HERA shows a breakdown of factorization both in normalization and in shape of the β dependence.

We thank the Fermilab staff and the technical staffs of the participating institutions for their vital contributions. This work was supported by the U.S. Department of Energy and National Science Foundation; the Italian Istituto Nazionale di Fisica Nucleare; the Ministry of Education, Science and Culture of Japan; the Natural Sciences and Engineering Research Council of Canada; the National Science Council of the Republic of China; the A. P. Sloan Foundation; the Max Kade Foundation; and the Ministry of Education, Science and Research of the Federal State Nordrhein-Westfalen of Germany.

[1] H1 Collaboration, T. Ahmed *et al.,* Phys. Lett. B **348**, 681 (1995); C. Adloff *et al.,* Z. Phys. C **76**, 613 (1997).
[2] ZEUS Collaboration, M. Derrick *et al.,* Z. Phys. C **68**, 569 (1995); Phys. Lett. B **356**, 129 (1995); Eur. Phys. J. C **6**, 43 (1999).
[3] UA8 Collaboration, A. Brandt *et al.,* Phys. Lett. B **297**, 417 (1992); **421**, 395 (1998).
[4] CDF Collaboration, F. Abe *et al.,* Phys. Rev. Lett. **78,** 2698 (1997); **79**, 2636 (1997); T. Affolder *et al.,* Phys. Rev. Lett. **84**, 232 (2000).
[5] We use rapidity and pseudorapidity, η, interchangeably; $\eta \equiv -\ln(\tan\frac{\theta}{2})$, where θ is the polar angle of a particle with respect to the proton beam direction. The azimuthal angle is denoted by ϕ, and the transverse energy of a jet, E_T^{jet}, is defined as $E^{\mathrm{jet}} \cdot \sin\theta$.
[6] See, for example, P. D. B. Collins, *An Introduction to Regge Theory and High Energy Physics* (Cambridge University Press, Cambridge, England, 1977).
[7] K. Goulianos, in *Proceedings of Vth International Workshop on Deep Inelastic Scattering and QCD, Chicago, 1997,* edited by J. Repond and D. Krakauer, AIP Conf. Proc. No. 407 (AIP, New York, 1997), pp. 527–532.
[8] L. Alvero, J. C. Collins, J. Terron, and J. Whitmore, Phys. Rev. D **59**, 074022 (1999).
[9] R. J. M. Covolan and M. S. Soares, Phys. Rev. D **60**, 054005 (1999); **61**, 019901(E) (2000).
[10] F. Abe *et al.,* Nucl. Instrum. Methods Phys. Res., Sect. A **271**, 387 (1988).
[11] F. Abe *et al.,* Phys. Rev. D **50**, 5518 (1994); **50**, 5535 (1994); **50**, 5550 (1994).
[12] F. Abe *et al.,* Phys. Rev. D **45**, 1448 (1992).
[13] M. Glück, E. Reya, and A. Vogt, Eur. Phys. J. C **5**, 461 (1998). The result does not depend significantly on the choice of parton density set.
[14] J. F. Owens, Phys. Rev. D **30**, 943 (1984).
[15] Armen Bunyatyan, Hannes Jung, and Chistophe Royon (private communication).
[16] K. Goulianos, Phys. Lett. B **358**, 379 (1995); **363**, 268 (1995).
[17] R. Enberg, G. Ingelman, and N. Timneanu, hep-ph/0001016.